Available online at www.elixirpublishers.com (Elixir International Journal)

Non-Linear Dynamics

Elixir Non-Linear Dynamics 99 (2016) 43221-43224

ISSN: 2229-712X

Experimental and Numerical Realization of Hyperchaos in a Four-Dimensional Autonomous Van Der Pol–Duffing Oscillator

S. Manimaran[1], V.Balachandran[2,*] and G. Kandiban[3]

[1]Department of Physics, Thanthai Hans Roever College, Perambalur - 621 212.

[2]Centre for Research-Department of Physics, Arignar Anna Government Arts College, Musiri, Tiruchirappalli - 621 211.

[3]Department of Physics, Vivekanandha College of Arts and Sciences for Women (Autonomous), Tiruchengode – 637 205.

ARTICLE INFO

Article history:

Received: 30 August 2016;

Received in revised form:

5 October 2016;

Accepted: 15 October 2016;

Keywords

Chaos,

Hyperchaos,

Four-dimensional autonomous Van der Pol–Duffing oscillator,

Power spectrum,

Hyperchaotic time series.

ABSTRACT

In this paper, we present the hyperchaotic dynamics of a four-dimensional autonomous Van der Pol–Duffing oscillator circuit. This circuit, which is capable of realizing the behavior of every member of Van der Pol–Duffing family, consists of just four linear elements (inductors and capacitors), a negative conductor and a cubic non-linear element. The route followed is a transition from regular behavior to Chaos and then to hyperchaos through period three-doubling bifurcation, as the system parameter is varied. The hyperchaotic dynamics, characterized by more than one positive Lyapunov exponents, is described by a set of four coupled first-order ordinary differential equations. This has been investigated extensively using laboratory experiments and numerical analysis.

1. Introduction

Chua's circuit is one of the best known and studied physical systems displaying chaotic behavior [1]. Its importance resides in allowing the investigation of a wide variety of non-linear phenomena using a simple experimental set-up. One of its main features is that the circuit non-linearity is continuous and piecewise-linear, with the breakpoints precisely established. This quality not only makes easier the theoretical analysis of the circuit properties but also makes more feasible the reproducibility of the experiments Chua's circuit has also technological importance, being an obvious choice in applications where electronic chaos generation is needed. One such application is secure communication systems. In this case it would be interesting if Chua's circuit could generate not only simple chaos (which is characterized by a single positive Lyapunov exponent) but also hyperchaos (characterized by at least two positive Lyapunov exponents). In fact, hyperchaos makes message masking more effective by giving rise to more complex time series [2-3].

At this point it is worth nothing that to produce hyperchaos has been the object of increasing interest. Its investigation is related to that of turbulence [4-5]. Theoretically discovered by Rossler, the first experimental detection of hyperchaos was achieved by Matsumoto et al., using an electrical circuit [6]. Since then, other similar experiments have been performed involving, e.g. electrical circuits, chemical reactions, semiconductors and lasers [7-10].

In this work we introduce a four-dimensional autonomous Van der Pol–Duffing oscillator circuit in order to make it hyperchaotic. By just including a one inductor is parallel to this canonical model and designing a simple cubic non-linear element, we are able to realize a very simple fourth-order non-linear dynamical system.

Without the parallel combination of one inductor, this circuit exhibits the familiar period-doubling route to chaos of the canonical model, as the control parameter (linear resistor (or) linear capacitor) as varied. However, an important noticeable feature is that when the parallel combination of one inductor (L_2) is included, the circuit exhibits period doubling route to chaos, periodic window and then hyperchaos through period three-doubling bifurcation, followed by boundary crisis.

The organization of the paper is as follows. In sec.2, we present details of the experimental realization of the four-dimensional autonomous Van der Pol–Duffing oscillator circuit and the occurrence of bifurcations leadings to chaos and hyperchaos, while in sec.3, the numerical simulation results of the circuit model is presented. In sec.4, we briefly summarize the results and suggest further improvements.

2. Experimental realization of the four-dimensional autonomous Van der Pol–Duffing oscillator

The original canonical Chua's circuit is one of the most simple third-order autonomous electronic generators of chaotic signals. It was synthesized using four linear element (two capacitors, C_1, C_2, one inductor, L_1, and resistor R) and two active elements (one linear negative conductor $-G_1$, and one cubic non-linear element namely parallel combination of two diodes) which can be built using off- the shelf op-amps. The chaotic behavior of the circuit was studied numerically, conformed mathematically and realized experimentally [11-12].

Varying the inductance L_1, while keeping the other circuit parameters at constant values, one finds that the circuit admits period-doubling bifurcations, intermittency and chaos [12], for a small range of inductance L_1, it also exhibits crisis induced intermittency [13].

Tele:

E-mail address: brsbala@rediffmail.com

In spite of these varied behavior, this circuit does not exhibits hyperchaos, because of its limited dimensionality. The important requisites for hyperchaos are (i) the minimal dimension of phase space that embeds the hyperchaotic attractor should be at least four energy storage elements, which requires the minimum number of coupled first–order ordinary differential equations to be four, and (ii) the number of terms in the coupled equations giving raise to instability should be at least two, of which one should be a non-linearity function [14].

By introducing an additionally one inductor L_2 in parallel to the negative conductor $-G_1$, the third-order canonical circuit it can be converted into a fourth-order autonomous electronic circuit and thereby made to exhibits strong hyperchaos. The four-dimensional autonomous Van der Pol–Duffing oscillator circuit satisfying the above criteria for hyperchaos is shown in Fig. 1. The characteristic of the negative conductance is mathematically represented by $i_{G1} = -G_1 V_2$ [15-19]. The characteristics of the cubic non-linear element are a three segment piecewise linearity, closely resembling that of a Chua's diode.

Applying Kirchoff's laws, the set of four coupled first–order differential equations describing the circuit is obtained as

$$C_1 \frac{dV_1}{dt} = i_{L_1} - i_N \tag{1}$$

$$C_2 \frac{dV_2}{dt} = G_1 V_2 - i_{L_1} - i_{L_2}$$

$$L_1 \frac{di_{L_1}}{dt} = V_2 - V_1$$

$$L_2 \frac{di_{L_2}}{dt} = V_2$$

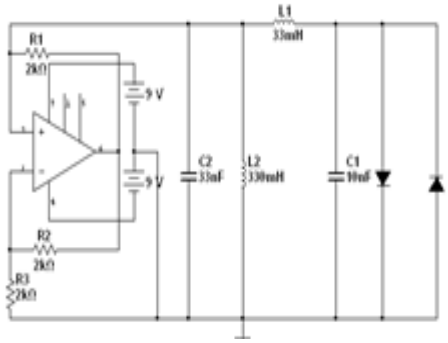

Fig 1. Circuit realization of the four-dimensional hyperchaotic autonomous Van der Pol Duffing oscillator circuit.

While V_1, V_2 are the voltages across the capacitors C_1, C_2 and i_{L_1}, i_{L_2} denotes the currents through the inductances L_1 and L_2 respectively. The term $i_N = g(V_1)$ representing the characterizes of the cubic non-linear element can be expressed mathematically as

$$g(V_1) = aV_1 + bV_1^3 \tag{2}$$

This higher dimensional circuit is also truly canonical. This is because, by removing the additional inductor (L_2) it exhibits all the behaviors reported by Chua and Lin (1991) and Kyprianidis (1995). When the additional inductor (L_2) is included it exhibits a regular behavior to Chaos and then to hyperchaos through boundary condition.

2.1. Experimental observations

Route to hyperchaos via period-doubling bifurcation

For our present experimental study we have chosen the following typical values of the circuit in Fig. 1(a): C_1 = 10 *nF*, C_2 = 33 *nF* and L_2 = 330 *mH*. The negative conductance and the cubic non-linear element are chosen to be the same as those of Kyprianidis *et al*., (1995), namely $-G_1$ = 0.5 *mS*, a = –1.25, b = 0.85 and Bp =1.0 *V*. Here the variable inductor, L_1 is assumed to be the control parameter. By increasing the value of L_1 from 5 *mH* to 45 *mH*, the circuit behavior of Fig.1 is found to transit from regular behavior to chaos and then to hyperchaotic attractor and boundary crisis, etc. When the value of L_1 is increased from 5 *mH* upto 45 *mH*, particularly in the range L_1 = 37.5 *mH* the system displays a hyperchaotic motion. The projected onto different planes formed by the V_1, V_2, i_{L_1} and i_{L_2} axes plane of simulation storage oscilloscope are shown in Fig. 2. Experimental time series were registered using a simulation storage oscilloscope for discrete values of C_1 and C_2 are shown if Fig. 3.

The distribution of power in a signal $x(t)$ is the most commonly quantified by means of the power density spectrum or simply power spectrum. It is the magnitude-square of the Fourier transform of the signal $x(t)$. It can be detect the presence of hyperchaos when the spectrum is broad-banded. The power spectrum corresponding to the voltages $V_1(t)$ and $V_2(t)$ waveforms across the capacitors C_1 and C_2 for the hyperchaotic regimes is shown in Fig. 4 which resembles broad-band spectrum noise.

3. Numerical Simulations

For a convenient numerical analysis of the experimental system given by Eqns. (1) we rescale the parameters as

$$V_1 = Vx_1, V_2 = Vx_2, i_{L_1} = \sqrt{\frac{C_1}{L_1}} V x_3, i_{L_2} = \sqrt{\frac{C_1}{L_1}} V x_4,$$

$$t = \sqrt{L_1 C_1}\,\tau,\ \alpha_1 = a\sqrt{\frac{L_1}{C_1}}, \alpha_2 = b\sqrt{\frac{L_1}{C_1}}, \upsilon = \frac{C_1}{C_2}, \gamma = G_1\sqrt{\frac{L_1}{C_1}}$$

$\beta = \frac{L_1}{L_2}$ and then redefine τ as T. Then the normalized equation of the four-dimensional autonomous Van der Pol–Duffing oscillator circuit (Fig.1) is

$$\dot{x}_1 = x_3 - \alpha_1 x_1 - \alpha_2 x_1^3 \tag{3}$$

$$\dot{x}_2 = \upsilon(\gamma x_2 - x_3 - x_4)$$

$$\dot{x}_3 = x_2 - x_1$$

$$\dot{x}_4 = \beta x_2$$

Where $g(x_1) = \alpha_1 x_1 + \alpha_2 x_1^3$ (4)

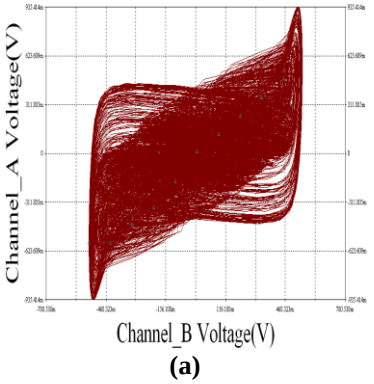

(a)

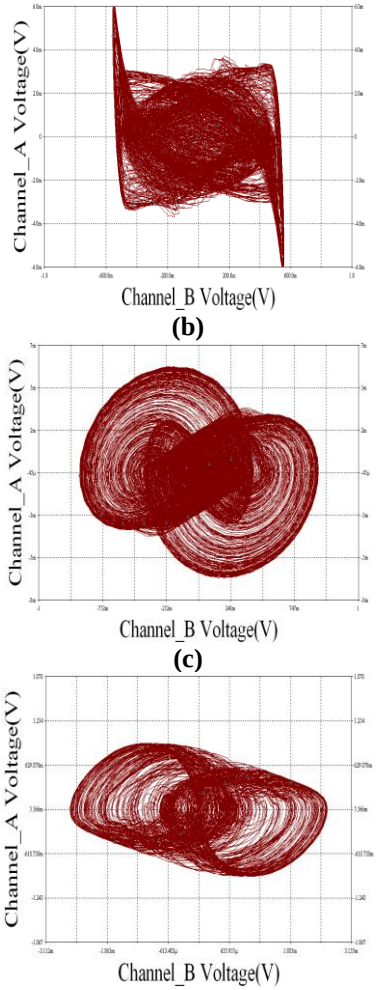

Fig 2. Simulation results of the projections of hyperchaotic attractor onto different planes.

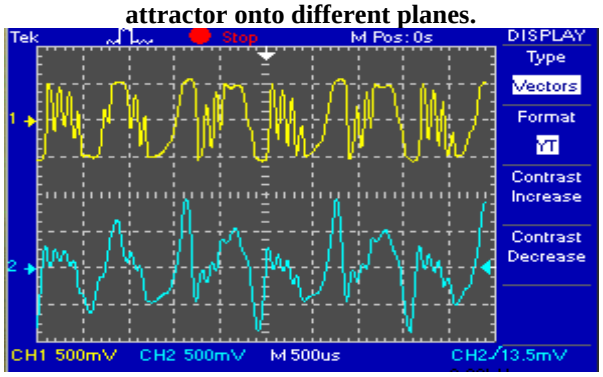

Fig 3. Simulation results of the hyperchaotic time series at fixed range of control parameter of L_1 = 37.5 mH.

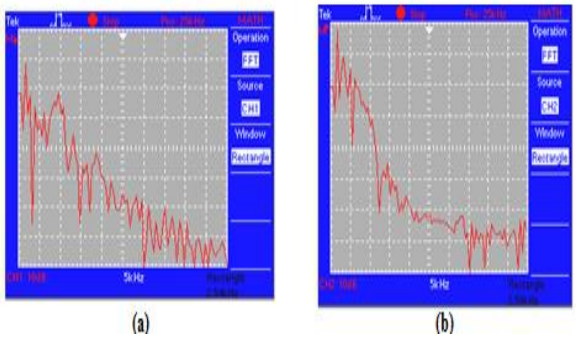

Fig 4. Simulation results of the hyperchaotic power spectrum at fixed range of control parameter of L_1 = 37.5 mH.

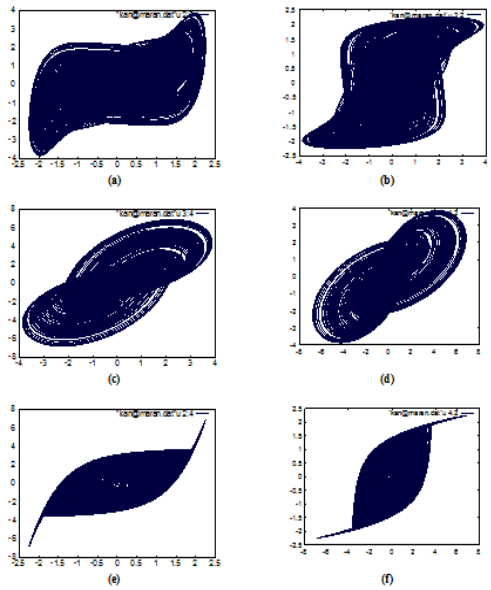

Fig 5. Hyperchaotic region observed from the circuit of Fig. 1. Projection onto different planes.

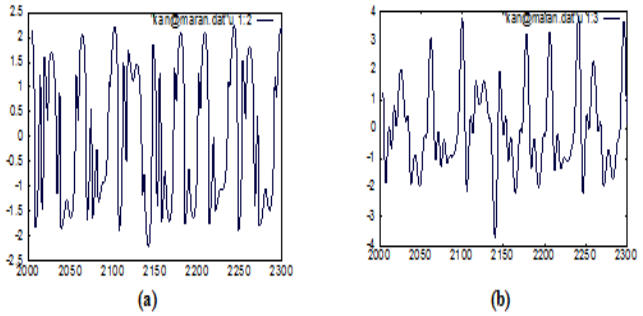

Fig 6. Numerical results of the hyperchaotic time series at fixed range of control parameter of L1 = 37.5 mH.

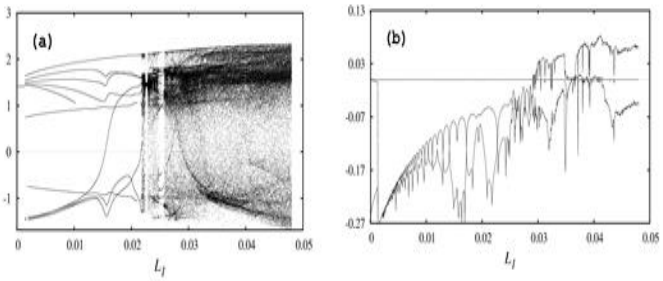

Fig 7(a). For the normalized Eq. (3): One parameter bifurcation diagram in the (L1 − x2) plane at fixed range of control parameter of L1 = (5 mH, 45 mH).

Fig 7(b). or the normalized Eq. (3): Two largest Lyapunov exponents versus L1 for two rajectories in the (L1− λ1, λ2) plane.

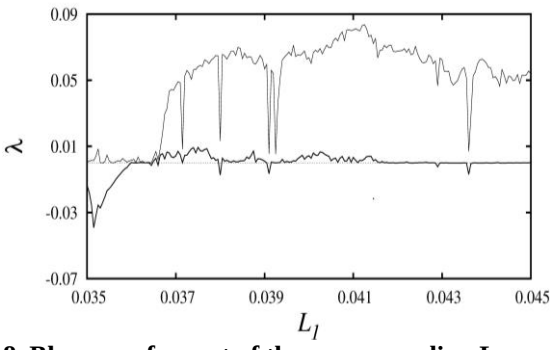

Fig 8. Blow-up of a part of the corresponding Lyapunov spectrum of Fig. 7(b).

As seen in Eqns. (3) and (4) can exhibits chaos and hyperchaos due to the existence of the nonlinear term $g(x_1)$ which is a piecewise-linear function with three segments. The dynamics of Eqns. (3) and (4) now depends upon the parameters $\alpha_1, \alpha_2, \upsilon, \gamma, \beta$, a = –1.25, b = 0.85 and V = 1. The experimental results have been verified by numerical simulation of the normalized Eqns. (3) and (4) using standard Runge-Kutta integration routine for a specific choice of system parameters employed in the laboratory experiments. That is, in the actual experimental setup the inductor L_1 is increased from 5 *mH* to 45 *mH*. Therefore, in the numerical simulation, we study the corresponding Eqns. (3) and (4) for L_1 in the range L_1 = (5 *mH*, 45 *mH*). When the value of L_1 is increased be high, particularly in the range L_1 = 37.5 *mH* the system displays a hyperchaotic motion. The projection of hyperchaotic attractors onto different planes are shown in Fig. 5. In Figure 6. Shows the numerical hyperchaotic time series was registered using a discrete value of 'L_1' serving as the control parameter. It is gratifying to note that the numerical results agree qualitatively very well with that of the experimental simulation results.

3.1. One parameter bifurcation diagram and Lyapunov exponents

The main features of the four-dimensional autonomous Van der Pol–Duffing oscillator circuit can be summarized in the one parameter bifurcation diagram drawn in the (L_1 − x_2) plane (Fig. 7 (a)). Note that x_2 is the rescaled variable in Eqns. (3), $x_2 = V_2/V$. This bifurcation diagram clearly indicates that in the region L_1 = (5 *mH*, 45 *mH*) the system undergoes period three-doubling bifurcation sequence to chaos, shows periodic windows through hyperchaotic region are observed in Fig. 1

The Lyapunov exponent's λ_1, λ_2, λ_3 and λ_4 were obtained using the Wolf algorithm. For periodic orbits $\lambda_1 = 0$, $\lambda_2, \lambda_3, \lambda_4 < 0$, for quasi-periodic orbits $\lambda_1 = \lambda_2 = 0$, $\lambda_3, \lambda_4 < 0$, while for chaotic attractor $\lambda_1 > 0$, $\lambda_2 = 0$, $\lambda_3, \lambda_4 < 0$ and for hyperchaotic attractor $\lambda_1 > \lambda_2 > 0$, $\lambda_3 = 0$, $\lambda_4 < 0$. The Lyapunov spectrum in the (L_1 − λ_1, λ_2) plane, that is the first two maximal Lyapunov exponents versus fixed range of the control parameter as L_1 is increased, is shown in Fig. 7 (b). This correlates to the bifurcation diagram, Fig 7 (a). In the range (45 *mH* > L_1 > 5 *mH*) the system exhibits periodic windows with no positive Lyapunov exponent. When L_1 is increased further in the range (45 *mH* > L_1 > 5 *mH*), the system becomes chaotic with a single positive Lyapunov exponent (λ_1).

The chaotic nature is also characterized by a single positive Lyapunov exponent (λ_1). It is quite fascinating to look at the window region in the range (45 *mH* > L_1 > 5 *mH*), which corresponds to an entirely different dynamical behavior. It has been observed that for L_1 > 5 *mH* the attractors of the system are in any one of the smooth regions of the piecewise segments. Correspondingly, the attractors exhibit one of the generic types of bifurcations, namely period-doubling, saddle-node, or hopf-bifurcations. A section of the bifurcation diagram and the Lyapunov spectrum for the range 45 *mH* > L_1 > 5 *mH* are shown in Figs. 7 (a) and 7 (b), respectively, for clarity. The Lyapunov spectrum in the (L_1–λ_1, λ_2) plane, that is the first two maximal Lyapunov exponents versus fixed range of the control parameter as L_1 is increased, is shown in Fig. 8. For the hyper chaotic attractor shown in Fig. 7 (b) for L_1 = 37.5 *mH* the Lyapunov exponents are λ_1 = 0.05962, λ_2 = 0.0089, λ_3 = −0.00024 and λ_4 = −4.54853.

4. Conclusions

It appears that the four-dimensional autonomous Van der Pol–Duffing oscillator circuit presented in this paper is one of the simplest fourth-order systems reported so far. Its simplicity arises from the fact that (i) the negative conductance is a simple op-amp impedance converter, (ii) the cubic non-linear element is synthesized from parallel combination of two diodes and (iii) the circuit equations are the most simple because of the inclusion of the inductor (L_2) is connected in parallel to the canonical Chua's circuit. When the value of L_1 is increased from 5 *mH* upto 45 *mH*, particularly in the range L_1 = 37.5 *mH* the system displays a hyperchaotic motion. The projected onto different planes formed by the V_1, V_2, i_{L_1} and i_{L_2} axes plane of simulation storage oscilloscope. The attractive feature of this circuit is the presence of strong hyperchaotic attractor over a range of parameter values, which might be useful for applications in controlling chaos and in secure communications.

It is of further interest to study these aspects also in this system as well as the torus breakdown route to chaos and synchronization of coupled hyperchaotic circuits of the present system of improved high security communication systems etc.

References

[1] R N Madan (ed.), *Chua's circuit: A Paradigm for Chaos*, (World Scientific, Singapore) (1993)
[2] J H Peng, E J Ding, M Ding and W Yang, *Phys. Rev. Lett.* 76, 904 (1996)
[3] L M Pecora, *Phys. Word.* 9, 17 (1996)
[4] D Ruelle, *Suppl. Progr. Theor. Phys*. 64, 339 (1978)
[5] O E Rossler, *Phys. Lett.* 71, 155 (1979)
[6] T Matsumoto and L O Chua, *IEEE Trans. Circuits. Syst.* CAS-33, 1143 (1986)
[7] A Tamasevicius, A Namajunas and A Cenys, *Electron. Lett.* 32, 957 (1996)
[8] K Thamilmaran, M Lakshmanan and A Venkatesan, *Int. J. Bifurcation and Chaos.* 14, 221 (2004)
[9] R Stoop, J Peinke, J Parisi, B Rohricht and R P Huebener, *Physica D*. 35, 425 (1989)
[10] R Vicent, J Dauden, P Colet and R Toral, *IEEE J. Quant. Electr*. 41, 541 (2005)
[11] Chua L O and Lin G N, *IEEE Trans. Circuits Syst.* 37, 885 (1990)
[12] L O Chua and G N Lin, *IEEE Trans. Circuits Syst.* 38, 510 (1991)
[13] L M Kyprianidis, M L Petrani, J A Kalomiros and A N Anagnostopoulos, *Phys. Rev. E*. 52, 2268 (1995)
[14] L Xian, W Jinzhi and H Lin, *Int. J. Bifurcation and Chaos.* 17, 2705 (2007).
[15] B Ruy, *Int. J. Bifurcation and Chaos.* 18, 1151 (2008)
[16] G P King and S T Gaito, *Phys. Rev. A.* 46, 3093 (1992)
[17] K Murali and M Lakshmanan, *Phys. Rev. E*. 45, 1624 (1993)
[18] V Balachandran and G Kandiban, *Indian J. Pure and Appl. Phys.* 47, 823 (2009)
[19] H B Fotsin and P Woafo, *Chaos, Solitons and Fractals.* 24, 363(2005).